



Petrography and Geochemical Signatures of Pegmatites from the Southeastern Part Comoé Basin (South-East Côte d'Ivoire, North Alépé)

**Martial Pohn Koffi Adingra^{a*}, Zié Ouattara^b,
Tokpa Kakeu Lionel Dimitri Boya^a, Augustin Junior Yapo^a,
Koffi Joseph Brou^a and Brice Roland Kouassi^c**

^a Laboratory of Geology, Mineral and Energy Resources, UFR-STRM, University Félix Houphouët-Boigny, 22 BP 582 Abidjan 22, Côte d'Ivoire.

^b Department of Geology and Materials, UFR Geological and Mining Sciences of University of Man, BP 20 Man, Côte d'Ivoire.

^c Department of Geosciences, UFR Biological Sciences, University Péléforo Gon Coulibaly, Côte d'Ivoire.

Authors' contributions

This work was carried out in collaboration among all authors. Author ZO manage field work and reviewed the work. Author TKLDB arranged comments and discussion of the study. Author AJY managed field work and XRF analysis. Author KJB arranged comments and XRF analysis. Author BRK performed XRF analysis. All authors read and approved the final manuscript.

Article Information

DOI: 10.9734/JGEESI/2023/v27i4680

Open Peer Review History:

This journal follows the Advanced Open Peer Review policy. Identity of the Reviewers, Editor(s) and additional Reviewers, peer review comments, different versions of the manuscript, comments of the editors, etc are available here: <https://www.sdiarticle5.com/review-history/98985>

Original Research Article

Received: 25/02/2023

Accepted: 30/04/2023

Published: 17/05/2023

*Corresponding author: E-mail: pohnmartial@yahoo.fr;

ABSTRACT

The pegmatitic rocks located in the south-east of Côte d'Ivoire between the Comoé basin and the Sefwi belt are the subject of this study. The geology of this region consists of gneisses, granites, microgranites, amphibolites, mylonites and metasediments. All these rocks are generally crosscut by quartz and pegmatite lodes. The petrographic studies allow us to discriminate four groups of pegmatites on the basis of mineralogy: (i) beryl-muscovite bearing pegmatite (Aboisso-Comoé), (ii) albite-tourmaline bearing pegmatite (Aboisso-Comoé), (iii) micas-tourmaline bearing pegmatite (Aloosso) and (iv) muscovite-garnet bearing pegmatite (Songan forest). XRD analyzes on 4 samples revealed the presence of lepidolite (lithium ore) in the muscovite-garnet bearing pegmatite (Songan forest) and phengite in beryl-muscovite bearing pegmatite (Aboisso-Comoé). The pegmatite diffractograms of Aboisso-Comoé (beryl-muscovite bearing pegmatite) and Songan forest (muscovite-garnet bearing pegmatite) show almost same signatures and would suggest that those pegmatites come from the same source. Geochemical analyzes by portable XRF carried out on muscovite and feldspar minerals indicate that the samples from Aboisso-Comoé and Songan forest have the characteristics of Lithium-Cesium-Tantalum type (LCT) pegmatites. The geochemical diagrams indicated the probable presence of beryl and spodumene type mineralization in the muscovite-garnet bearing pegmatite.

Keywords: Comoé Basin; Côte d'Ivoire; petrography; geochemistry; pegmatites; LCT.

1. INTRODUCTION

According to London [1], "pegmatites are rocks that are essentially magmatic in origin, predominantly granitic in composition and considered to be the most differentiated on earth". The pegmatites are sources of raw materials such as industrial minerals (quartz, feldspathoids, corundum, micas, phosphates, etc), gemstones and rare metals (Li, Rb, Cs, REE, U, Zr, Nb, Ta, etc.) [2]. Indeed, pegmatites are the main source of strategic metals, indispensable elements used in new technologies (electric vehicles, solar panels, batteries, wind turbines, etc). According to [3], pegmatites are grouped into five classes on the basis of the pressure and temperature conditions of their emplacement and enrichment trends in trace elements. Based on this classification, we find: the abyssal pegmatites (AB), muscovite bearing pegmatites (Ms), muscovite and rare elements bearing pegmatites (Ms-REL), rare elements pegmatites (REL) as well as the miarolitic pegmatites (MI). Another classification is based on the geochemical signature of the pegmatites (trace element enrichment), which is strongly related to the mineralogy, but also to the geochemical nature of the associated granites [3-6]. It comprises three families designated by the elements enriched in pegmatites: Lithium-Cesium-Tantalum (LCT) family, Niobium-Yttrium-Fluorine (NYF) family and mixed LCT+NYF family. The genesis of these rocks is explained by two

distinct models: the partial melting model of a protolith [7-12] and the magmatic differentiation model of a granite parent [13,7,14,1,15-17]. In Côte d'Ivoire, Precambrian pegmatites have been studied through scientific and mineral exploration work (Adam, SODEMI, Côte d'Ivoire, Unpublished results); [18,19]. Fifteen zones of interest have been identified throughout Côte d'Ivoire [20]. Two zones of interest are located in the south-east of Côte d'Ivoire around Agboville and Alépé towns. The present study will focus on the pegmatites of the Alépé area, precisely to the north of this town. Adam's work (SODEMI, Côte d'Ivoire, Unpublished results) in this area indicates the presence of two types of pegmatite: muscovite-biotite-oligoclase bearing pegmatites and tourmaline-beryl-microcline bearing pegmatites. Except the work of Adam [20], very few studies have been carried out on the pegmatitic rocks of this part of Côte d'Ivoire. It is in this context that the present study is developed with the general objective to improve geological knowledge of the pegmatites in the south-eastern part of Côte d'Ivoire (north of Alépé). The specific objectives are (i) to identify the mineralogy and petrography of the pegmatites in the south-eastern part of the Comoé Basin, (ii) to determine the geochemical characteristics of muscovites and feldspars from pegmatites studied by portable XRF and (iii) to highlight the potential mineralization of the pegmatites in the south-eastern part of the Comoé Basin.

1.1 Geological Context

1.1.1 Regional geology

The study area is located in the south-eastern part of Côte d'Ivoire. This country is located in the southern part of the West African Craton, more precisely at the Leo-Man shield (Fig. 1A). The geology of Côte d'Ivoire is marked by two main areas: the sedimentary basin (2.5% of territory) and the Precambrian basement (97.5% of territory). The basement is consisted of two domains separated by the Sassandra Fault [21,22]: a nucleus with Archean age (3600-2500 Ma) located at the western part of the fault and a domain with Paleoproterozoic age (2500-1800 Ma), also called the Baoulé-Mossi domain, located at the east of fault. This Paleoproterozoic domain is made up of so-called Birimian formations [23,22,24-28]. Birimian rocks are essentially consisted of greenstone belts and birimian basins, all intruded by several generations of granitoids [29-31,25,27,32]. A total of seventeen birimian volcano-sedimentary belts have been identified in Côte d'Ivoire [33,34]. According to some authors [24,35-37,30,26,27,38], the sedimentary basins are mainly siliciclastic, composed of turbidite mudstones and grauwackes; the latter being occasionally carbonated. However, some basins may also contain significant amounts of volcanoclastics, as well as subordinate volcanic rocks and chemical sediments, including manganese deposits [39-41,26,42]. The geological units of the Comoé Basin consist of a terrigenous sedimentary series including phyllitic matrix sandstones, arkoses and pelitic layers [43-45]. Several granitoid plutons intrude these metasedimentary series [45-47]. The study area is marked by metamorphism ranging from greenschist to amphibolite facies [36,30,42,47]. The pegmatitic rocks are heterogeneously distributed on the Man-Leo shield. Several studies conducted on the Man-Leo shield have identified rare metal pegmatites:

- In Burkina Faso, sodic and quartz-feldspathic pegmatites with cassiterite, spodumene, tourmaline, garnet and apatite have been reported in the Zorgho-Zoungou locality [48]. The pegmatites with cassiterite, colombo-tantalite, tourmaline, garnet, beryl, muscovite and quartz are observed in the locality of Kankounadéni at the northern end of the Ferkéssédougou

granite batholith [48]. To this must be added the rare metal pegmatites of Mangodara (southwestern Burkina Faso) hosted in the granite-gneiss complex [49];

- In Mali, lithium occurrences associated with spodumene bearing pegmatites have been identified in the localities of Bougouni and Goulamina. These pegmatites are intrusive in granites and their metasedimentary host rocks [50,51];
- In southwestern part of Ghana, pegmatites have been identified in the localities of Saltpond, Mandkwazi and Winneba. They are intrusive in metavolcanic, metasedimentary and granitic rocks. These pegmatites contain rare metal bearing minerals such as cassiterite, columbite-tantalite, ixiolite, and rutile [52].
- In Côte d'Ivoire, studies on pegmatites come from the work of SODEMI (Adam, SODEMI, Côte d'Ivoire, Unpublished results) [2] which defined 15 areas of interest throughout the country. The pegmatites of the Issia locality (Centre-Ouest) have been the subject of several studies [18,19,53]. The pegmatites of this locality are hosted and around 3 generations of granites (G1, G2 and G3). Some of the granites and pegmatites would be the source of the Issia columbite-tantalite deposit.

1.1.2 Local geology

The Comoé Birimian Basin or Comoé Unit, deformed during the Eburnean orogeny, is one of the most important Birimian formations in the West African craton [44]. It covers the following countries: Côte d'Ivoire, Burkina (known as the Houndé Basin) and Ghana (known as the Sunyani Basin). In Côte d'Ivoire, this basin is subdivided into two units: (i) the Haute-Comoé unit (in the northern part of Dabakala up to the Burkina-Faso border) and (ii) the Comoé unit s.s (the Abengourou-Dimbokro group in the central-eastern and southeastern part of Côte d'Ivoire) [33]. The study area is located in the southeastern part of the Comoé unit s.s. The lithology of Comoé unit s.s consist of a terrigenous sedimentary series comprising sandstones with phyllitic matrix, arkoses and pelitic layers [43,37,45]. In addition, the work of [47] identified other lithologies including micaschists, mylonites, paragneisses and metawackes. These rocks mainly have shale compositions and weakly sandstone

compositions, with protoliths having a predominance for the mafic pole [47]. Several weakly metamorphosed granitoid plutons (metamonzogranites, metagranites and metagranodiorites) intrude the metasediments (metarenites and metasilstones) [35] (Fig. 1B).

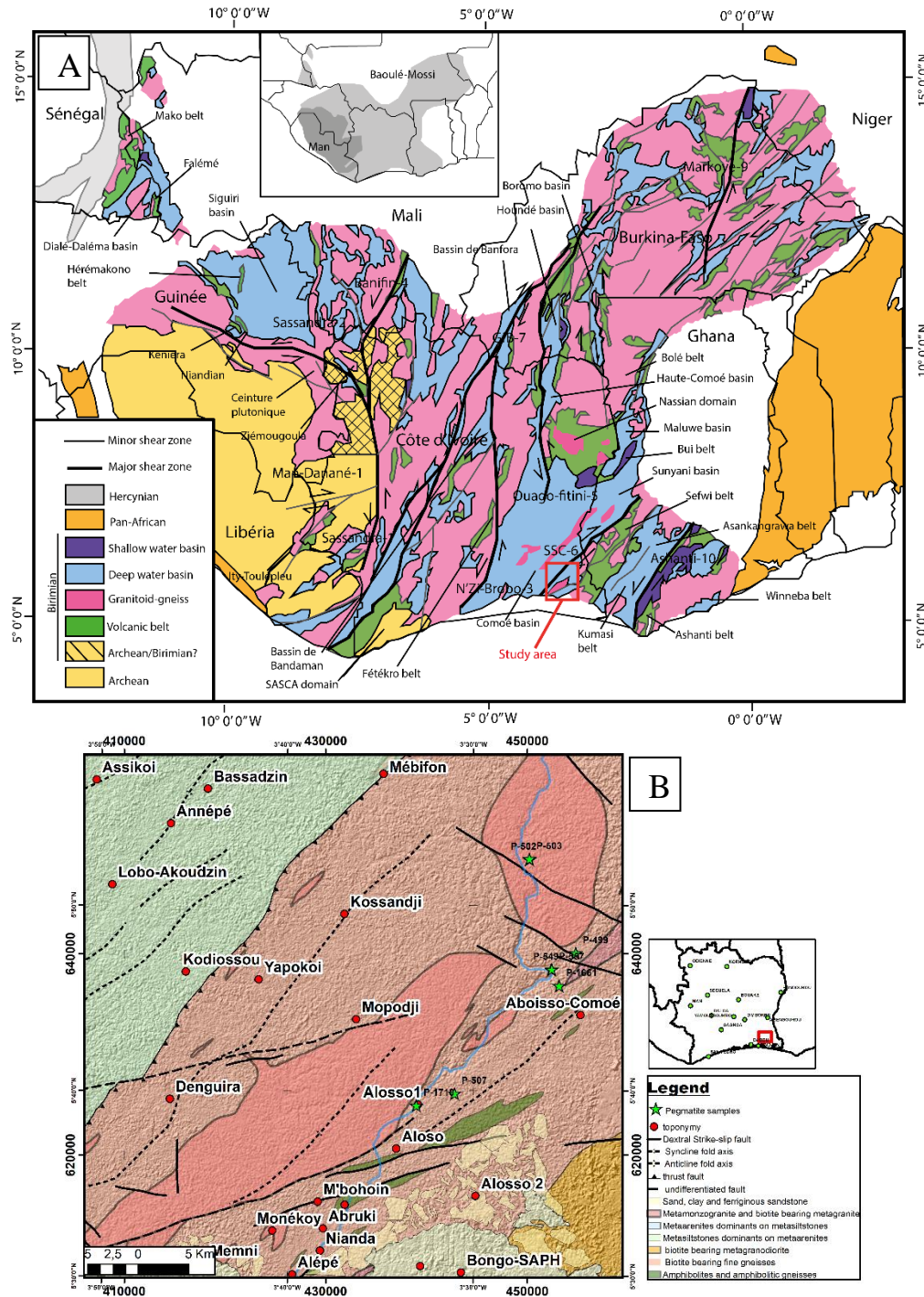


Fig. 1. Regional and local geology of study area
 (A): Schematic geological map of the Man-Leo shield showing the study area [28]; (B): Geological map of the study area at 1:200 000 with samples location [45]

All the geological formations mentioned above are intersected by several pegmatites and quartz lodes. The work carried out by [1] in the area study distinguishes two main types of pegmatites: calc-alkaline pegmatites with biotite-oligoclase-muscovite intrusion in paragneiss and tourmaline-beryl-microcline bearing pegmatites. All those geological units were affected by polyphase deformation: D1, D2, D3 and D4 [35,45,37,25,38]. The metamorphism is mainly from greenschist facies. It reaches amphibolite facies conditions around the leucogranite plutons [54,55,42].

2. METHODOLOGY

To achieve these specific objectives, the methodology was carried out in three stages: petrographic observations, whole rock XRD analysis and portable XRF analysis for muscovite and feldspar minerals.

2.1 Macroscopic and Microscopic Petrography Study

This stage required field work which consisted of geological surveys in the study area. The following criteria were used to describe the rocks and provide it the name: mode of outcropping, color, structure, texture, degree of weathering, magnetic test, mineralogical composition. Additional observations have been done in the Geology, Mineral and Energy Resources Laboratory on the samples collected in order to clarify certain minerals and assess their abundance in the rock. Samples have been located on the geological map (Fig. 1B). Microscopic studies have been performed in the same laboratory with OPTIKA microscope.

2.2 Portable XRF Analysis

The chemistry of some pegmatite minerals was obtained using the Niton XL3t GOLDD+ portable X-ray fluorescence analyzer. The principle of X-ray fluorescence is to bombard matter with X-rays, the matter re-emits energy in the form of X-rays. The X-ray spectrum emitted by the material is characteristic of the composition of the sample. Within the framework of this study, measurements were obtained on the feldspar and muscovite minerals of the pegmatites, at the Geology, Mineral Resources and Energy Laboratory. In view of the large size of these minerals, the measurements are carried out directly on the rock. The compositions obtained

are extracted from the device using NDT 8.2.1 software and sorted, converted with Excel sheet.

2.3 X-ray Diffractometer Analysis

The X-ray diffractometer analysis was carried out at the scientific center of the University Félix Houphouët Boigny at Bingerville. The principle is as follows: the X-ray beams produced by the tube are sent onto the sample (rock powders) in which they are deflected by the atoms. These diffracted beams interfere with each other, leading to the production of an intense signal in specific areas of space. This signal is collected by the detector and plotted as a curve (diffractogram). X-ray diffraction is based on the recording of a diffractogram and the analysis of its peaks in order to characterize the crystals present in the sample from the following elements:

- position of peaks: qualitative analysis, identification of the crystalline phases present;
- peak widths: size, crystallite shape and internal stresses;
- peak intensity: chemical composition estimation, quantitative analysis and preferential orientation.

A total of 4 pegmatite samples (P-502, P-503, P-1661 and P-549) were analyzed using this method.

3. RESULTS AND DISCUSSION

3.1 Results

The main results obtained take into account the petrographic data, the XRD and XRF analysis.

3.1.1 Petrography of pegmatites

The petrographic study allows us to group the pegmatites according to mineralogy into 4 groups: (i) micas-tourmaline bearing pegmatite, (ii) albite-tourmaline bearing pegmatite, (iii) beryl-muscovite bearing pegmatite, (iv) muscovite-garnet bearing pegmatite. These pegmatites are found in various types of host rocks: gneisses, micaschists, amphibolites and granitoids. The pegmatites studied can also be grouped according to locality: Aboisso-Comoé pegmatites, Alosso pegmatites and Songan forest pegmatites.

3.1.1.1 Alosso pegmatites

- Micas-tourmaline bearing pegmatite

The samples collected are the following: P-507, P-1718 and P-1710. This pegmatite outcrops as dislocated blocks near Alosso in a cocoa plantation. The rock is weakly weathered, massive, leucocratic color with the following mineralogical composition: quartz (40%), orthoclase (25%), other feldspars (10%), biotite (10%), muscovite (10%) and black tourmaline (5%) (Fig. 2A&B).

3.1.1.2 Songan forest pegmatites

In this part of the study area, no pegmatite had been observed according to previous works. The petrographic study identified a muscovite-garnet bearing pegmatite.

- Muscovite-garnet bearing pegmatite

Observed in the Songan forest, this pegmatite with a leucocratic color outcrops in the form of a boudin lode-oriented NW-SE hosted in a garnet bearing micaschist (Fig. 2C&D) and also like dislocated blocks. This pegmatite orientation is concordant with the schistosity of the host rock. The mineralogical composition consists of quartz (45%), feldspar (30%), muscovite (20%) and garnet (5%).

3.1.1.3 Aboisso-Comoé pegmatites

Two types of pegmatites have been observed in the vicinity of this locality. These are beryl-muscovite bearing pegmatites and albite-tourmaline bearing pegmatites.

- Albite-tourmaline bearing pegmatite

This pegmatite (sample P-1661) outcrops as dislocated blocks at 200 m from the mouth of the Comoé and Malamasso rivers in a cocoa plantation. Rock is massive, leucocratic color, graphitic texture (Fig. 2E&F) with the blocks showing a N40° orientation. The graphitic texture is typical of granitic pegmatites. This cuneiform texture is due to the inter-growth of quartz and alkali feldspar, it's a typical edge texture in granitic pegmatites. The mineralogical composition is: quartz 40%, albite 30%, other feldspars 20%, muscovite 5% and accessory black tourmaline.

- Beryl-muscovite bearing pegmatite

This pegmatite (sample P-549) outcrops in the form of dislocated blocks or intrusive lodes in

micas bearing granites near the mouth between Comoé and Malamasso rivers (Fig. 3A&B). Leucocratic in color and affected by a schistosity oriented N127°, this pegmatite has the following mineralogical composition: quartz (40%), feldspar (35%) and muscovite (15%) with accessory apatite, black tourmaline and green pale beryl mineral.

Microscopic observation allowed to describe in more details some minerals. Muscovite occurs as subhedral to euhedral (some megacrystal with size up to 1 cm), elongate, oriented and deformed (Fig. 3C&D). They marked the schistosity in the rock. Muscovite is associated with the anhedral quartz mineral showing undulating extinction. In the fracture plane, small subhedral tourmaline is visible (size less than 200 µm) (Fig. 3D). Hexagonal euhedral beryl mineral (size around 0.8mm) with imperfect cleavage planes shows some fractures (Fig. 3E&F). Beryl is often associated with muscovite and quartz and exhibit some muscovite inclusion.

3.1.2 Mineral abundance and zonation of the pegmatites studied

The petrographic study revealed the mineralogical composition of the pegmatites studied. The main minerals observed are: quartz, feldspars, muscovites, biotites, tourmalines, apatites and garnets. The Table 1 shows the abundance of the different minerals in the pegmatites studied. They are generally rich in quartz and feldspar. Muscovite is generally present in all the pegmatites studied with a pronounced abundance in the central and northern parts of the study area (samples from Aboisso-Comoé and Songan forest). The biotites are located in the pegmatites of the southern part of the study area (the Alosso samples). Tourmalines are found in the localities of Alosso and Aboisso-Comoé, i.e. in the southern and central parts of the study area. The pegmatites of Aboisso-Comoé are the only ones to contain apatite minerals. According to [55], pegmatites can be grouped into two families according to the temperature of crystallisation of the minerals: low temperature pegmatites (paragenesis: muscovite, muscovite-beryl, muscovite-albite, muscovite-spodumene and spodumene-lepidolite-albite) and high-temperature pegmatites (paragenesis: feldspar, biotite-magnetite, biotite-muscovite, biotite-tourmaline-muscovite and tourmaline-muscovite). In view of the mineralogical abundance, it is possible to

establish the following zonation: the pegmatites of northern part (Songan forest) are rather low-temperature while those in the southern zone

(Alosso) are high-temperature. Both families have been found in the pegmatites of Aboisso-Comoé.

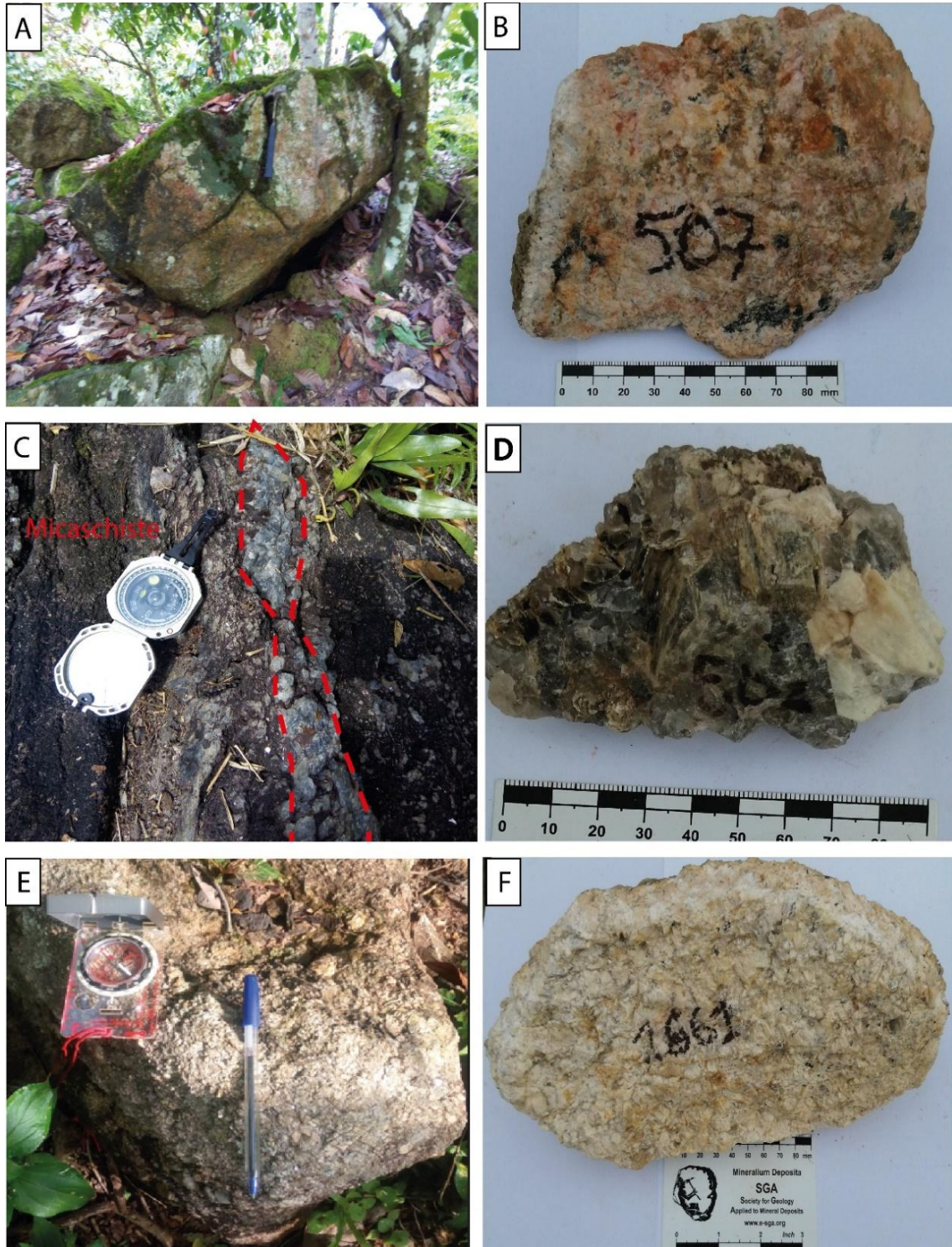


Fig. 2. Macroscopic aspects of the southeastern part Comoé basin pegmatites
(A)&(B): Mica-tourmaline bearing pegmatite of Alosso outcrop and hand specimen sample; (C)&(D): Muscovite-garnet bearing pegmatite from Songan forest; (E)&(F): Albite-tourmaline bearing pegmatite from Aboisso-Comoé showing graphitic texture

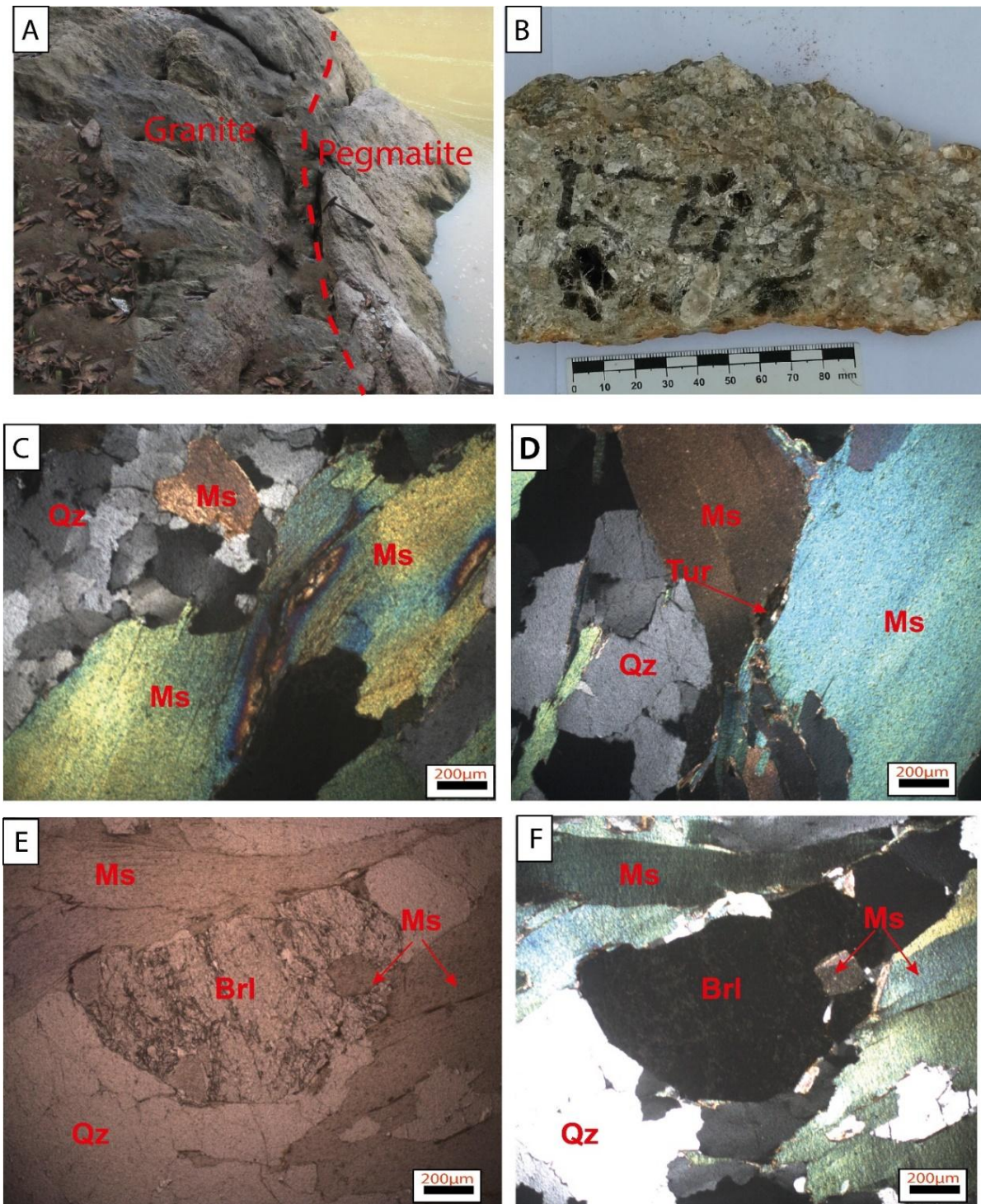


Fig. 3. Macroscopic and microscopic aspects of beryl-muscovite bearing pegmatite from Aboisso-Comoé

(A)&(B): Outcrop and hand specimen of beryl-muscovite bearing pegmatite; (C): subhedral muscovite mineral deformed associated with anhedral quartz showing undulating extinction; (D): tourmaline in fracture plane border of muscovite mineral; (E): hexagonal beryl mineral with imperfect cleavages in LPNA; (F): hexagonal beryl mineral with imperfect cleavages in LPA

Brl: Beryl; Ms: Muscovite; Qz: Quartz; Tourmaline: Tur

3.1.3 DRX analysis of the pegmatites studied

The X-ray diffraction analysis helped to confirm the presence of some minerals identified during the petrographic study and at the same time highlighted some unidentified minerals. Four diffractograms were made from samples P-1661, P-549, P-502 and P-503. The different diffractograms results are presented below:

- the diffractogram of sample P-1661 (Albite-tourmaline bearing pegmatite from Aboisso-Comoé) shows the presence of quartz, albite and andesine. It therefore confirms the presence and the abundance of the albite in this pegmatite (Fig. 4A);
- The diffractogram of sample P-549 (Beryl-muscovite bearing pegmatite from Aboisso-Comoé) indicates the presence of quartz, muscovite and phengite (Fig. 4B). The presence of phengite is an indicator of the setting conditions of this pegmatite. Indeed, this mineral is typical of high-pressure metamorphism zones. The importance of the schistosity planes observed within this pegmatite is also an indication that it was formed under high pressure conditions;
- The diffractogram of sample P-502 (Muscovite-garnet bearing pegmatite from Songan forest) highlights crystalline phases such as quartz, muscovite and lepidolite (Fig. 4C). The presence of lepidolite (lithium ore) is an excellent indicator for lithium exploration in this part of the study area;
- The sample P-503 diffractogram is quite similar to sample P-502 (Fig. 4D). The same mineral phases have been identified (quartz-muscovite-lepidolite). These two samples located in the Songan forest, are about 100 metres apart. This diffractogram therefore confirms the interest in exploring for lithium ore in this part of the study area.

The diffractograms of sample P-549, P-502 and P-503 show almost the same patterns although the minerals are different in some points (Fig. 4B, C & D). The difference is observed in some peaks which are marked by the presence of muscovite or lepidolite (in the diffractograms of P-502 and P-503) rather than the phengite (in diffractogram P-549). All those observations may be suggesting that the pegmatites P-549, P-502 and P-503 would come from the same source. We can also suggest that due to metasomatism process or high pressure and temperature, the

lepidolite and/or muscovite is replaced by the phengite in beryl-muscovite bearing pegmatites deformed (P-549).

3.1.4 Geochemistry of pegmatite minerals with portable XRF

The geochemical characteristics of some pegmatite minerals were studied from the chemistry obtained by portable XRF. This study was conducted exclusively on muscovite and feldspar minerals. A total of 5 muscovite samples (PM-549, PM-557; PM-502; PM-503; PM-1710) and 3 feldspar samples (PF-1661; PF-502; PF-1718) located in the vicinity of Aboisso-Comoé, Alosso and in the Songan forest were analyzed.

3.1.4.1 Trace element concentrations

The contents of trace elements are recorded in Table 2. Elements such as Ba, Cs, Sr and Rb could be quantified in all samples while elements such as Ni, Co, Cr, Hf, Nb, Ni, Sb, Sc, Ta, Ti, Th, U, Zn and Zr could not be detected in all minerals.

Ta was detected in 3 muscovite samples (PM-549, PM-503 and PM-1718) with concentrations of 150, 270 and 50 ppm respectively. The highest concentration was observed in sample PM-503 from the Songan forest. Nb was also detected in PM-549 and PM-503 with concentrations of 30 and 50 ppm respectively. Ta levels are higher than Nb levels in PM-549 ($Nb/Ta = 0.2$) and PM-503 ($Nb/Ta = 0.18$). Rb contents vary between 47 and 2697 ppm in the muscovite samples. Maximum values are observed in samples PM-503 (2697 ppm) and PM-502 (1830 ppm) and PM-549 (899 ppm). In the feldspar samples, Rb concentrations range from 9 to 149 ppm. As for Cs, it varies between 51 and 187 ppm for muscovite minerals and from 37 to 546 ppm for feldspar minerals. The highest concentrations are observed in samples PF-502 (546 ppm) for feldspar and PM-502 (187ppm) for muscovite. The K/Rb ratio of muscovites is an excellent indicator for the degree of fractionation. This ratio varies from 26.27 to 91.52 in the muscovites studied. The lowest values are identified in muscovites PM-502 (38.77) and PM-503 (26.27) from the Songan forest.

All this information indicates that the Songan and Aboisso-Comoé pegmatites have geochemical characteristics close to LCT pegmatites (LILE abundance and $Ta > Nb$).

3.1.4.2 Typology of the pegmatites studied

The K/Rb vs Rb diagram of [56] was used to differentiate barren from mineralized pegmatites. This diagram indicates that two samples PM-557 (Aboisso-Comoé) and PF-502 (Songan pegmatite) are in field of mineralized pegmatites (Fig. 5A). The K/Rb versus Cs diagram [57] applied to feldspars and muscovites also allows to distinguish barren from mineralized pegmatites (Fig. 5B). It also led to specify the type of mineralization. The diagram applied to the muscovites shows that the Songan pegmatites are found in the field of beryl type for PM-503 and at the boundary between beryl type and spodumene subtype for PM-502 (Fig. 5C). Sample PM-557 (Aboisso-Comoé pegmatite) is located at the boundary between barren and beryl mineralized pegmatites. The same

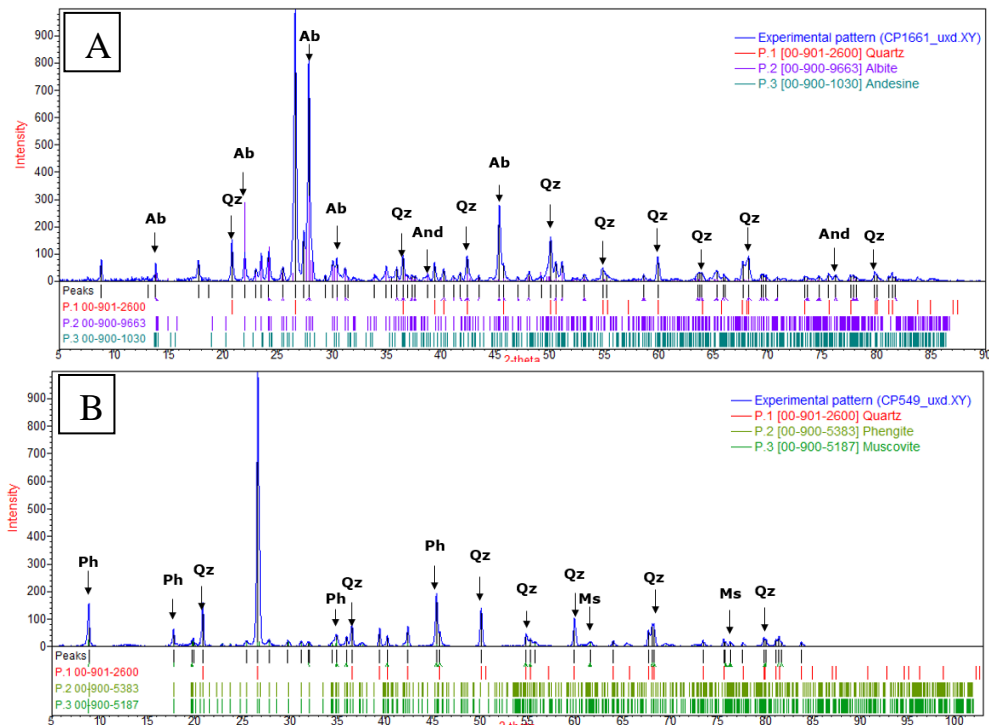
diagram applied to the feldspars indicates that sample PF-502 belongs to the field of pegmatites mineralized in beryl and spodumene type.

The Rb versus Sr diagram of [58] gives an indication of the distance to the source plutons (Fig. 5D). This diagram indicates that samples PM-502, PM-503 and PM-549 are the furthest from the source at about 30 km. This diagram confirms the results obtained from the diagrams of [56] and [57] for the mineralization of the Songan forest samples (PM-502 and PM-503). Indeed, the distance from the source is an excellent factor contributing to the evolution and mineralisation of pegmatites. The different diagrams used highlight the mineralization potential of the Songan and Aboisso Comoé samples.

Table 1. Abundance of minerals in the pegmatites studied

| Samples | Localities | Mineralogy | | | | | | | |
|---------|---------------|------------|-----|-----|----|-----|----|-----|-----|
| | | Qtz | Fsp | Ms | Bt | Tur | Ap | Grt | Brl |
| P-507 | Aloso | ++ | +++ | - | + | ++ | - | - | - |
| P-1718 | Aloso | ++ | ++ | + | + | + | - | - | - |
| P-1661 | Aboisso-Comoé | +++ | ++ | + | - | + | + | - | - |
| P-549 | Aboisso-Comoé | +++ | ++ | ++ | - | + | + | - | + |
| P-502 | Songan forest | +++ | ++ | ++ | - | - | - | + | - |
| P-503 | Songan forest | ++ | ++ | +++ | - | - | - | - | - |

Qtz: Quartz; Fsp: Feldspar; Ms: Muscovite; Bt: Biotite; Tur: Tourmaline; Ap: Apatite; Grt: Garnet; Brl: Beryl



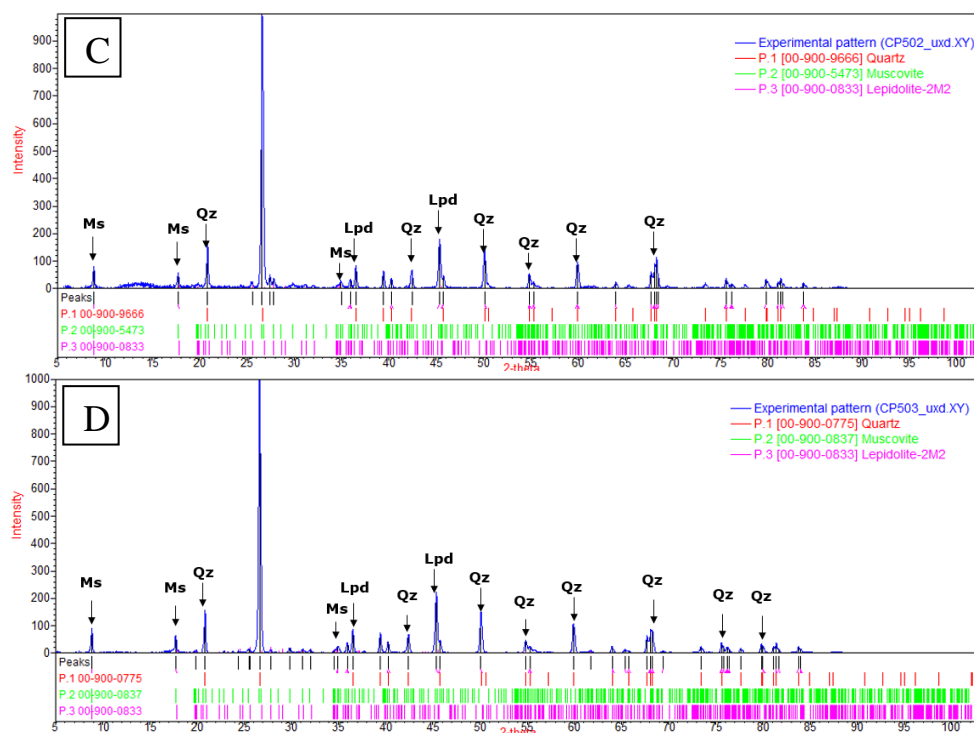


Fig. 4. The different diffractograms of the pegmatites of Aboisso-Comoé and Songan sites (A): diffractogram of sample P-1661; (B): diffractogram of sample P-549; (C): diffractogram of sample P-502; (D): diffractogram of sample P-503. Qtz: quartz; Ms: Muscovite; Ab: Albite; And: Andesine; Lpd: Lepidolite; Ph: phengite

Table 2. Trace (ppm) element concentrations of muscovites and feldspars in pegmatites of studied area

| Chemical elements | Muscovites | | | | | Feldspars | | |
|-------------------|------------|--------|---------|---------|---------|-----------|---------|--------|
| | PM-549 | PM-557 | PM-502 | PM-503 | PM-1710 | PF-1661 | PF-1718 | PF-502 |
| | AC | AC | SO | SO | AL | AC | AL | SO |
| As | < LOD | < LOD | < LOD | < LOD | < LOD | < LOD | < LOD | < LOD |
| Ba | 637.51 | 481.92 | 279.98 | 356.23 | 358.88 | 305.86 | 309.85 | 261.18 |
| Co | 98.56 | < LOD | < LOD | < LOD | < LOD | < LOD | < LOD | < LOD |
| Cr | < LOD | 88.59 | < LOD | < LOD | < LOD | < LOD | < LOD | 13.51 |
| Hf | < LOD | 40.00 | < LOD | 110.00 | < LOD | < LOD | < LOD | < LOD |
| Nb | 30.00 | < LOD | < LOD | 50.01 | < LOD | < LOD | < LOD | < LOD |
| Ni | 102.37 | < LOD | 149.22 | 120.19 | 110.01 | 46.69 | < LOD | 78.52 |
| Cs | 51.92 | 72.08 | 187.89 | 80.99 | 51.47 | 37.78 | 53.81 | 546.54 |
| Rb | 899.80 | 47.86 | 1830.69 | 2697.87 | 506.09 | 149.59 | 9.74 | 51.99 |
| Sr | 13.39 | 119.28 | 20.11 | 29.74 | 5.88 | 23.58 | 42.22 | - |
| Sb | 21.21 | 64.26 | 25.66 | < LOD | < LOD | 32.55 | 46.13 | 63.29 |
| Sc | < LOD | < LOD | < LOD | < LOD | < LOD | < LOD | 13.95 | 23.24 |
| Ta | 150.02 | < LOD | < LOD | 270.03 | 50.01 | < LOD | < LOD | < LOD |
| Th | 6.03 | < LOD | < LOD | < LOD | < LOD | 7.30 | 5.27 | < LOD |
| Ti | 1718.03 | 104.43 | 518.50 | 429.38 | 2078.62 | 289.48 | < LOD | 874.18 |
| U | < LOD | 6.68 | < LOD | < LOD | < LOD | < LOD | < LOD | < LOD |
| Zn | 61.48 | 16.24 | 246.82 | 336.51 | 38.70 | 32.42 | < LOD | 155.71 |
| Zr | < LOD | < LOD | < LOD | < LOD | 2.78 | < LOD | < LOD | < LOD |
| K/Rb | 91.52 | 81.53 | 38.77 | 26.27 | 93.21 | 163.32 | 236.87 | 40.23 |

Elements in ppm; AC: Aboisso-Comoé; Al: Alosso; SO: Songan

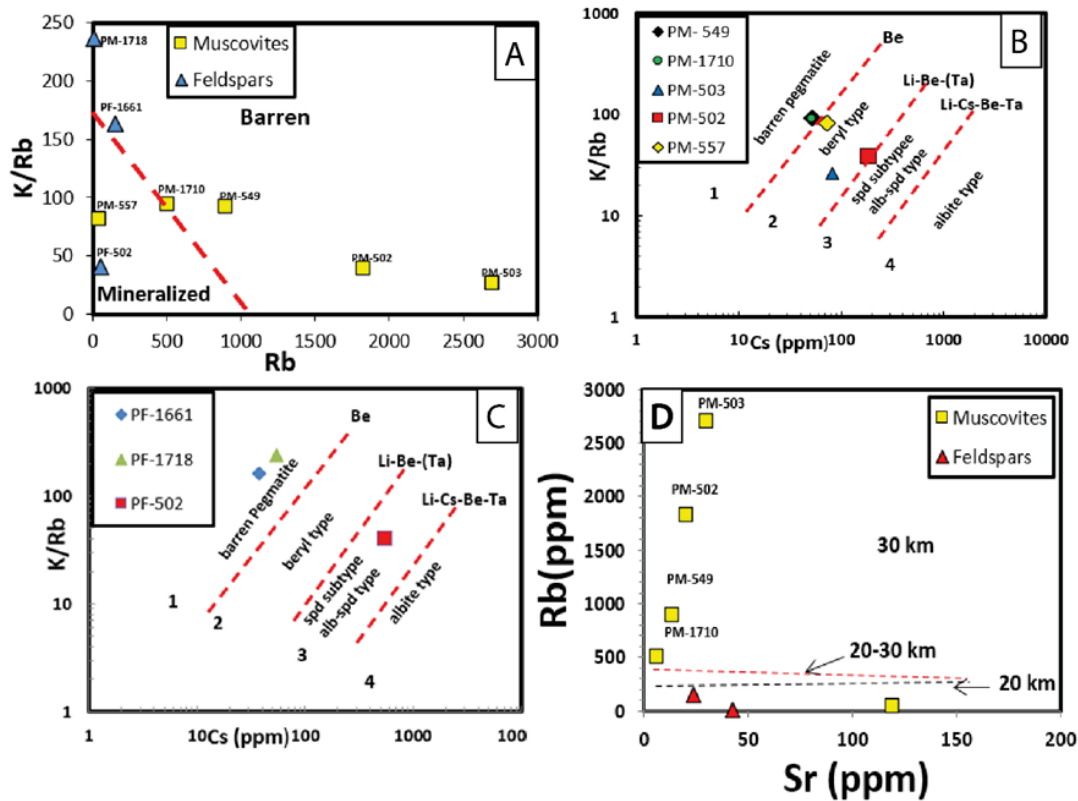


Fig. 5. Geochemical diagrams applied to muscovites and feldspars from pegmatites south-eastern part of Comoé Basin

(A) : *K/Rb versus Rb diagram [56] applied to muscovites and feldspars from pegmatites of south-eastern part Comoé basin;*(B): *K/Rb versus Cs diagram [57] applied to the muscovites from pegmatites of south-eastern part Comoé basin;*(C): *K/Rb versus Cs diagram [57] applied to feldspars from pegmatites of south-eastern part Comoé basin;* (D): *Rb versus Sr diagram [58] applied to muscovites and feldspars from pegmatites of south-eastern part Comoé basin*

3.2 Discussion

The present work has identified several groups of pegmatites according to mineralogy. These are: beryl-muscovite bearing pegmatite, albite-tourmaline bearing pegmatite, micas-tourmaline bearing pegmatite and muscovite-garnet bearing pegmatite. They can also be grouped into two distinct families according to the mineral crystallization temperatures: (i) low temperature pegmatites or “cold pegmatites” and (ii) high temperature pegmatites or “hot pegmatites”. The results of [20] in the Alépé region had indicated the presence of these two groups with a predominance for the hot pegmatites. According to this author, their host rocks are essentially metamorphic rocks. The present study has also highlighted the presence of metamorphic rocks (micaschists, gneiss, etc.). Nevertheless, in the Aboisso-Comoé area, beryl-muscovite bearing pegmatite is observed in a two-mica bearing granite.

Metasediments are regularly referred to as protoliths of LCT-type rare metal pegmatites, or in terms of rare metal reservoirs [7-12]. The presence of metasediments in the study area and particularly the discovery of muscovite-garnet bearing pegmatite concordant with the schistosity of the host rock garnet bearing micaschists (Songan Forest) are excellent observations on the para-derived origin of the pegmatites in this part of the study area.

The presence of albite and lepidolite in Aboisso-Comoé and Songan forest pegmatites, could indicate that their belonging to the rare metal pegmatite class and the REL-Li subclass as described by authors such as [59,3,60]. According to [61], pegmatites belonging to the complex type albite-spodumene and albite are the most evolved and have the particularity of being the most lithium-rich.

The diffractograms indicated that the beryl-muscovite bearing pegmatite from Aboisso-

Comoé and the muscovite-garnet bearing pegmatite from Songan forest, may come from the same source. The diffractograms also show the possible replacement of muscovite or lepidolite by phengite in the beryl-muscovite bearing pegmatite from Aboisso-Comoé. This replacement seems to be linked to the metamorphism which affected this pegmatite. The replacement of muscovite by phengite known as Tschermark substitution has been described by many authors [62 to 66]. The temperature or pressure controlled contribute to change the chemical composition of muscovite. Muscovites from Aboisso-Comoé and Songan forest samples show enrichments in LILEs (Cs, Rb, K...). Micas composition in LILEs is used to define trace element enrichment trends for evolved granites and pegmatites [8,67-71,53].

The Nb/Ta and K/Rb ratios in the muscovites of the Songan Forest pegmatites are low. Both ratios in micas are known to decrease with melt fractionation after a Rayleigh-type fractionation model [72,67,68,69]. These ratios confirm that the pegmatites of the Songan Forest are the most evolved.

The Lithium-Cesium-Tantalum (LCT) family is characterised by an enrichment in the alkaline elements Li, Cs, Ta over Nb, Be, P and F generally hosted by spodumene/petalite, minerals of the lepidolite, pollucite and columbite group [16]. The Songan forest and Aboisso-Comoé pegmatites have geochemical characteristics close to the LCT type pegmatites (abundance of LILE and Ta>Nb). This type of pegmatite has also been identified by several authors [73,74,75,18,19,51] in the Paleoproterozoic domain of the West African Craton as rare metal pegmatites (Saraya in Senegal, Winneba in Ghana, Issia in Côte d'Ivoire, Goulamina in Mali). They are generally spodumene mineralized.

4. CONCLUSION

This petrogeochemical study on the pegmatites of the southeastern part of the Comoé basin has made it possible to distinguish them. According to Petrographic studies, 4 types of pegmatites have been identified: beryl-muscovite bearing pegmatites (Aboisso-Comoé), albite-tourmaline bearing pegmatites (Aboisso Comoé), muscovite-garnet bearing pegmatites (Songan forest) and micas-tourmaline bearing pegmatites (Alosso). XRD analysis revealed the presence of:

- lepidolite in muscovite-garnet bearing pegmatites (Songan forest);
- phengite in beryl-muscovite bearing pegmatites (Aboisso-Comoé);
- albite and andesine in albite-tourmaline pegmatites (Aboisso-Comoé).

The diffractograms of Songan and Aboisso-Comoé showed almost the same signature and would suggest that they are coming from the same source. The replacement of lepidolite or muscovite by the phengite in beryl-muscovite bearing pegmatites is may be due to the metamorphism.

The chemistry of feldspars and muscovites analyzed by portable XRF in the Songan (PM-502 and PM-503) and Aboisso-Comoé (P-549) pegmatites indicate that these minerals are rich in LILEs (Cs, K, Rb...) and have a Nb/Ta<1 ratio. The Songan and Aboisso-Comoé pegmatites have geochemical characteristics close to LCT pegmatites (abundance of LILE and Ta>Nb). The geochemical diagrams indicate the presence of probable beryl and/or spodumene mineralization for the Songan pegmatite. According to geochemistry results, muscovite-garnet bearing pegmatite from Songan forest seems to be the more evolved pegmatites in this region.

ACKNOWLEDGEMENTS

Special thanks to scientific pole of the University Félix Houphouët Boigny at Bingerville and Miss Sikely Ivanne (XRD analysis) (for XRD analysis) and Geology, Mineral Resources and Energy Laboratory (for microscopic studies and XRF analysis).

COMPETING INTERESTS

Authors have declared that no competing interests exist.

REFERENCES

1. London D. Ore-forming processes within granitic pegmatites. *Ore Geology Reviews*. 2018;101:349-83. Available: 10.1016/j.oregeorev.2018.04.020
2. Dill HG. Pegmatites and aplites: Their genetic and Applied ore geology. *Ore Geol Rev*. 2015;69:417-561. Available:10.1016/j.oregeorev.2015.02.022

3. Cerny P, Ercit TS. The classification of granitic pegmatites revisited. *Can Mineral.* 2005;43(6):2005-26.
Available:10.2113/gscanmin.43.6.2005
4. Cerny P. Rare-element granitic pegmatites. Part I: Anatomy and internal evolution of pegmatitic deposits. *Geosci Can.* 1991a;49-67.
5. Cerny P. Rare-element granitic pegmatites. Part II: Regional to global environments and petrogenesis. *Geosci Can.* 1991b;18:2.
6. Wise MA, Müller A, Simmons WB. A proposed new mineralogical classification system for granitic pegmatites. *Can Mineral.* 2022;60(2):229-48.
Available:10.3749/canmin.1800006
7. Shearer CK, Papike JJ, Jolliff BL. Petrogenetic links among granites and pegmatites in the Harney Peak rare-element granite-pegmatite system, Black Hills, South Dakota. *Can Mineral.* 1992;30(3):785-809.
8. Van Lichtervelde M, Grégoire M, Linnen RL, Béziat D, Salvi S. Trace element geochemistry by laser ablation ICP-MS of micas associated with Ta mineralization in the Tanco pegmatite, Manitoba, Canada. *Contrib Mineral Petrol.* 2008;155(6):791-806.
Available:10.1007/s00410-007-0271-z
9. Simmons W, Falster A, Webber K, Roda-Robles E, Boudreaux AP, Grassi LR, et al. Bulk composition of Mt. Mica pegmatite, Maine, USA: implications for the origin of an LCT type pegmatite by anatexis. *Can Mineral.* 2016;54(4):1053-70.
Available:10.3749/canmin.1600017
10. Shaw RA, Goodenough KM, Roberts NMW, Horstwood MSA, Chenery SR, Gunn AG. Petrogenesis of rare-metal pegmatites in high-grade metamorphic terranes: A case study from the Lewisian gneiss Complex of north west Scotland. *Precambrian Res.* 2016;281:338-62.
Available:10.1016/j.precamres.2016.06.008
11. Turlin F, André-Mayer AS, Moukhsil A, Vanderhaeghe O, Gervais F, Solgadi F, et al. Unusual LREE-rich, peraluminous, monazite- or allanite-bearing pegmatitic granite in the central Grenville Province, Quebec. *Ore Geol Rev.* 2017;89:627-67.
Available:10.1016/j.oregeorev.2017.04.019
12. Fuchsloch WC, Nex PAM, Kinnaird JA. Classification, mineralogical and geochemical variations in pegmatites of the Cape Cross-Uis pegmatite belt, Namibia. *Lithos.* 2018;296-299:79-95.
Available:10.1016/j.lithos.2017.09.030
13. Jahns RH, Burnham CW. Experimental studies of pegmatite genesis; I, A model for the derivation and crystallization of granitic pegmatites. *Econ Geol.* 1969;64(8):843-64.
Available:10.2113/gsecongeo.64.8.843
14. Mahood GA, Nibler GE, Halliday AN. Zoning patterns and petrologic processes in peraluminous magma chambers: Hall Canyon pluton, Panamint Mountains, California. *GSA Bull.* 1996;108(4):437-53.
Available:10.1130/0016-7606(1996)108<0437:ZPAPPI>2.3.CO;2
15. Cerny P, London D, Novak M. Granitic pegmatites as reflections of their sources. *Elements.* 2012;8(4):289-94.
Available:10.2113/gselements.8.4.289.
16. Breiter K, Ďurišová J, Hrstka T, Korbelová Z, Vašinová Galiová M, Müller A, et al. The transition from granite to banded aplite-pegmatite sheet complexes: An example from Megiligar Rocks, Tregonning topaz granite, Cornwall. *Lithos.* 2018;302-303:370-88.
Available:10.1016/j.lithos.2018.01.010
17. Galliski MÁ, Márquez-Zavalía MF, Pagano DS. Metallogenesis of the Totoral LCT rare-element pegmatite district, San Luis, Argentina: A review. *J S Am Earth Sci.* 2019;90:423-39.
Available:10.1016/j.jsames.2018.12.018
18. Allou AB. Factors, parameters, distribution dynamics and genesis of columbo-tantalite deposits from Issia, central-western Côte d'Ivoire (PhD). Montreal: University of Quebec at Chicoutimi. 2005;369.
19. Brou KJ. Petrogenetic evolution of the Issia granite complex (Centre-West of Côte d'Ivoire) and associated Nb-Ta deposits [thesis] [thesis] University Félix Houphouët Boigny, UFR STRM. 2021; 272.
20. Adam H. The pegmatites of the Eburnean geosyncline in Côte d'Ivoire [PhD thesis]. Abidjan: Univ., Fac. Sc. 1969;178.
21. Bessoles B. Geology of Africa. *Bur.Rech. Geol. Min. Same. The West African Craton.* 1977;88:1: 402.

22. Lemoine S. Geological evolution of the Dabakala region (NE of the Ivory Coast) in the Proterozoic. Possibilities of extension to the rest of Ivory Coast and Burkina Faso: similarities and differences; the Greenville-Ferkessédougou and Grand Cess-Niakaramandougou lineaments. Doctorate of Science. Ferrand: University Cl. 1988;388.
23. Camil J. Petrography, chronology of Archean assemblages and associated formations in the Man region (Côte d'Ivoire). Implications for the geological history of the West African craton [doctoral thesis], ès Sci.Uni. from Abidjan, Ivory Coast. 1984;306.
24. Milési JP, Feybesse JL, Ledru P, Dommangeat A, Ouedraogo MF, Tegye M, et al. Gold mineralization in West Africa and its litho-structural evolution in the Lower Proterozoic. Chron Min Res. 1989;497:3-98.
25. Feybesse JL, Billa M, Guerrot C, Duguey E, Lescuyer JL, Milési JP, et al. The Paleoproterozoic of Ghanaian province: Geodynamic model and ore controls, including regional stress modeling. Precambrian Res. 2006;149(3-4):149-96.
Available:10.1016/j.precamres.2006.06.003
26. Pouclet A, Doumbia S, Vidal M. Geodynamic setting of the Birimian volcanism in central Ivory Coast (western Africa) and its place in the Palaeoproterozoic evolution of the Man shield. Bull Geol Soc Fr. 2006;177(2):105-21.
Available:10.2113/gssgfbull.177.2.105
27. Baratoux L, Metelka V, Naba S, Jessell MW, Grégoire M, Ganne J. Juvenile Paleoproterozoic crust evolution during the Eburnean orogeny (~2.2-2.0 ga), Western Burkina Faso. Precambrian Res. 2011;191(1-2):18-45.
Available:10.1016/j.precamres.2011.08.010
28. Greenholm M. The Birimian event in the Baoulé Mossi domain (West African Craton) – regional and global context. PhD. Univ. Lund. 2014;116.
29. Liégeois JP, Claessens W, Camara D, Klerkx J. Short-lived Eburnean orogeny in southern Mali. Geology, tectonics, U-Pb and Rb-Sr geochronology. Precambrian Res. 1991;50(1-2):111-36.
Available:10.1016/0301-9268(91)90050-K
30. Doumbia S, Pouclet A, Kouamelan A, Peucat JJ, Vidal M, Delor C. Petrogenesis of juve-nile-type Birimian (Paleoproterozoic) granitoids in central Côte d'Ivoire, West Africa: Geochemistry and geochronology. Precambrian Res. 1998;87(1-2):33-63.
Available:10.1016/S0301-9268(97)00201-5
31. Gasquet D, Barbey P, Adou M, Paquette JL. Structure, Sr-Nd isotope geochemistry and zircon U-Pb geochronology of the granitoids of the Dabakala area (Côte d'Ivoire): Evidence for a 2.3 ga crustal growth event in the Paleoproterozoic of West Africa. Precambrian Res. 2003; 127(4):329-54.
Available:10.1016/S0301-9268(03)00209-2
32. Sakyi PA, Addae RA, Su B-X, Dampare SB, Abitty E, Su BC, et al. Petrology and geochemistry of TTG and K-rich Paleoproterozoic Birimian granitoids of West African Craton (Ghana): Petrogenesis and tectonic implications. Precambrian Res. 2020;336:105492.
Available:10.1016/j.precames.2019.105492
33. Tagini B. Structural sketch of the Ivory Coast [University of Lausanne thesis] and SODEMI publication. 1971;302.
34. Yacé I. Eburnean volcanism in the central and southern parts of the Precambrian chain of Fettekro in Côte d'Ivoire [state Doctorate thesis]. University of Abidjan. 1976;373.
35. Milési JP, Ledru P, Feybesse JL, Dommangeat A, Marcoux E. Early Proterozoic ore deposits and tectonics of the Birimian orogenic belt, West Africa. Precambrian Res. 1992;58(1-4):305-44.
Available:10.1016/0301-9268(92)90123-6
36. Hirdes W, Senger R, Adjei J, Efa E, Loh G, Tettey A. Explanatory notes for the geological map of southwest Ghana 1. Asafo. 1993;100(000): sheets Wiawso (0603D):(0603C), kukuom (0603B). Goaso. Sunyani (0703D) & Berekum (0703C). Geol Jahrb B;83: 139p:(0603A).
37. Vidal M, Alric G. The Paleoproterozoic (Birimian) of Haute-Comoé, in the West African Craton in Côte d'Ivoire: a transtensional back-arc basin. Precambrian Res. 1994;65(1-4):207-29.

- Available:10.1016/0301-9268(94)90106-6
38. Adingra MPK. Petro-structural and geochemical characterization of the Birimian formations of the south-eastern part of the Comoé basin (north of Alépé south-eastern Côte d'Ivoire): implications for geodynamic evolution [doctoral thesis in earth science]. Félix Houphouët Boigny University Côte d'Ivoire. 2020;221.
 39. Leube A, Hirdes W, Mauer R, Kesse GO. The early proterozoic birimian supergroup of Ghana and some aspects of its associated gold mineralization. *Precambrian Res.* 1990;46(1-2):139-65.
Available:10.1016/0301-9268(90)90070-7
 40. Mortimer J. Lithostratigraphy of the early proterozoic toumodi volcanic group in central Côte d'Ivoire: implications for Birrimian stratigraphic models. *J Afr Earth Sci.* 1992b;14(1):81-91.
Available:10.1016/0899-5362(92)90057-J
 41. Mücke A, Dzigbodi-Adjimah K, Annor A. Mineralogy, petrography, geochemistry and genesis of the Paleoproterozoic Birimian manganese formation of Nsuta/Ghana. *Mineral Deposita.* 1999;34(3):297-311.
Available:10.1007/s001260050205
 42. Vidal M, Gumiaux C, Cagnard F, Pouclet A, Ouattara G, Pichon M. Evolution of a Paleoproterozoic "weak type" orogeny in the West African Craton (Ivory Coast). *Tectonophysics.* 2009;477(3-4):145-59.
Available:10.1016/j.tecto.2009.02.010
 43. Alric G, Guibert P, Vidal M. The problem of the Birrimian greywackes of Côte d'Ivoire: A review and new data. The case of the Comoé unit. series II(7). SC: CR Academy. Paris, t. 304. 1987;289-94.
 44. Vidal M. Eburnean deformations of the Birimian unit of Comoé (Ivory Coast). *J Afr Earth Sci.* 1987;6(2):141-52.
Available:10.1016/0899-5362(87)90056-X
 45. Delor C, Diaby I, Tastet JP, Yao B, Siméon Y, Vidal M, et al. Explanatory note for the geological map of the Ivory Coast 1/200000, sheet of Grand Bassam. Ministry of mines and energy. Abidjan, Ivory Coast: DMG. 1992;30.
 46. Jessell MW, Amponsah PO, Baratoux L, Asiedu DK, Loh GK, Ganne J. Crustal-scale transcurrent shearing in the Paleoproterozoic Sefwi-Sunyani-Comoé region, West Africa. *Precambrian Res.* 2012;212-213:155-68.
Available:10.1016/j.precamres.2012.04.015
 47. Adingra MPK, Coulibaly Y, Ouattara Z, Coulibaly I. Petrographic and geochemical characteristics of the metasediments of the southeastern part of the Birimian basin of the Comoé (north of Alépé-southeast of the Côte d'Ivoire) *RAMRES Review.* 2018;06(2):28-35.
 48. Castaing C, Billa M, Milési J, Thiéblemont D, Le Metour J, Egal E, et al. Explanatory note for the geological and mining map of Burkina Faso at 1:1,000,000. BRGM BUMIGEB. 2003;147.
 49. Wilédio M-EB. Origin, evolution and rare metal mineralization of West African pegmatites [single doctoral thesis]. University of Toulouse. 2022;3:432.
 50. Bassot JP, Traoré H, Méloux J. Explanatory note of the 1/1,500,000 geological map of the Republic of Mali. Ministry of Industrial Development and Tourism, National Directorate of Geology and Mines; 1981.
 51. Wilde A, Otto A, McCracken S. Geology of the Goulamina spodumene pegmatite field, Mali. *Ore Geol Rev.* 2021; 134:104162.
Available:10.1016/j.oregeorev.2021.104162
 52. Adams S. Rare metals mineralization of Winneba-Mankoadze pegmatites, South Western Ghana [Master's thesis]. University of Ghana; 2013.
 53. Brou JK, Van Lichtervelde M, Kouamelan NA, Baratoux D, Thébaud N. Petrogenetic relationships between peraluminous granites and Li-Cs-Ta rich pegmatites in south Issia zone (Central-West of Côte d'Ivoire): Petrography, Mineralogy, Geochemistry and zircon U-Pb Geochronology. *Mineral Petrol.* 2022;116(6):443-71.
Available:10.1007/s00710-022-00790-2
 54. Guibert Ph, Vidal M. Un modèle d'évolution structurale du Birrimien du Sud-Est de la Côte d'Ivoire. *Ann. Univ. Abidjan, série C (sciences)*, t. 1984;XX:277-293.
 55. Fersman AE. Pegmatites. 3rd ed. Vol. 1. Moscow, Leningrad: USSR Academy of Sciences Publishing. 1940;712.

56. Staurov OD, Stolyarov LS, Isochewa EI. Geochemistry and origin of verkh iset granitoid massif in central Ural. *Geochem Int.* 1969;6:1138-46.
57. Trueman DL, Cerny P. Exploration for rare-element granitic pegmatites. In: *Granitic pegmatites in science and industry*. Mineralogical Association of Canada, short course handbook. 1982;8:463-93.
58. Condie KD. Trace element geochemistry of Archean granite rocks from the Barberton Region, South Africa, AM. *Mineral. Earth Planet Sci Lett.* 1976;29:389-400.
59. Ginsburg A, Timofeyev I, Feldman L. Principles of geology of the granitic pegmatites. Mosc: Nedra. 1979;296.
60. Ercit TS. Identification and alteration trends of granitic-pegmatite-hosted (Y, REE, U, Th)– (Nb, Ta, Ti) oxide minerals: A statistical approach. *Can Mineral.* 2005;43(4):1291-303.
Available:10.2113/gscanmin.43.4.1291
61. Deveaud S. Characterization of the emplacement of LCT-type rare element pegmatite fields: representative examples of the variscan chain (phdthesis). University of Orléans. 2015;321.
62. Guidotti CV, Sassi FP. Petrogenetic significance of Na-K white mica mineralogy. Recent advances for metamorphic rocks. *Eur J Mineral.* 1998;10(5):815-54.
Available:10.1127/ejm/10/5/0815
63. Leoni L, Sartori F, Tamponi M. Compositional variation in K-white micas and chlorites coexisting in Al-saturated metapelites under late diagenetic to low-grade metamorphic conditions (Internal Liguride Units, Northern Apennines, Italy). *Eur J Mineral.* 1998;10(6):1321-40.
Available:10.1127/ejm/10/6/1321
64. Velde B. Phengite micas: synthesis, stability, and natural occurrence. *Am J Sci.* 1965;263(10):886-913.
Available:10.2475/ajs.263.10.886
65. Vidal O, Parra T. Exhumation paths of high pressure metapelites obtained from local equilibria for chlorite-phengite assemblages. *Geol J.* 2000;35(3-4):139-61.
Available:10.1002/gj.856
66. Vidal O, Parra T, Trotet F. A thermodynamic model for FeMg aluminous chlorite using data from phase equilibrium experiments and natural pelitic assemblages in the 100-600. C. 1–25. kbar range. *Am J Sci.* 2001;6(301):557-92.
Available:10.2475/ajs.301.6.557
67. Martins T, Roda-Robles E, Lima A, de Parseval P. Geochemistry and evolution of micas in the Barroso–Alvão pegmatite field, Northern Portugal. *Can Mineral.* 2012;50(4):1117-29.
Available:10.3749/canmin.50.4.1117
68. Stepanov AS, Hermann J. Fractionation of Nb and Ta by biotite and phengite: Implications for the "missing Nb paradox". *Geology.* 2013;41(3):303-6.
Available:10.1130/G33781.1
69. Stepanov A, Mavrogenes JA, Meffre S, Davidson P. The key role of mica during igneous concentration of tantalum. *Contrib Mineral Petrol.* 2014;167(6):1009.
Available:10.1007/s00410-014-1009-3
70. Hulsbosch N, Boiron MC, Dewaele S, Muchez P. Fluid fractionation of tungsten during granite–pegmatite differentiation and the metal source of peribatholithic W quartz veins: Evidence from the Karagwe-Ankole Belt (Rwanda). *Geochim Cosmochim Acta.* 2016;175:299-318.
Available:10.1016/j.gca.2015.11.020
71. Chukwu A. Geochemical characterization of mineralized pegmatites around wowyen areas, Akwanga, Northcentral Nigeria. *Adv Geol Geotech Eng Res.* 2022;4(1):37-48.
Available:10.30564/agger.v4i1.4314
72. Cerny P, Burt D. Paragenesis, crystallochemical characteristics, and geochemical evolution in micas in granite pegmatites. *Micas.* 1984;257-97.
73. Ndiaye PM, Dia A, Vialette Y. New petrographic, geochemical and geochronological data on Paleoproterozoic granitoids of the Dialé-Daléma supergroup (Senegal Oriental): Petrogenetic and geodynamic implications. *J Afr Earth Sci.* 1997;25:193-208.
Available:10.1016/S0899-5362(97)00098-5
74. Dampare SB, Nyarko BJB, Osa S, Akaho EHK, Asiedu DK, Serfor-Armah Y, et al. Simultaneous determination of tantalum, niobium, thorium and uranium in placer columbite-tantalite deposits from the Akim Oda District of Ghana by epithermal instrumental neutron activation analysis. *J Radioanal Nucl Chem.* 2005;265(1):53-9.

- Available:10.1007/s10967-005-0860-0
75. Nude P, Hanson J, Dampare S. Geochemistry of pegmatites associated with the cape coast granite complex in the Egyaa and Akim Oda areas of Southern Ghana. Ghana J Sci. 2011;51:89-100.

© 2023 Adingra et al.; This is an Open Access article distributed under the terms of the Creative Commons Attribution License (<http://creativecommons.org/licenses/by/4.0>), which permits unrestricted use, distribution, and reproduction in any medium, provided the original work is properly cited.

Peer-review history:
The peer review history for this paper can be accessed here:
<https://www.sdiarticle5.com/review-history/98985>